Tailoring Silicon Oxycarbide Glasses for Oxidative Stability

F. I. HURWITZ AND M. A. B. MEADOR
NASA Lewis Research Center, Cleveland, OH44135

frances.hurwitz@lerc.nasa.gov
maryann.meador@lerc.nasa.gov

Abstract. Blackglas™ polysiloxane systems produce silicon oxycarbide glasses by pyrolysis in inert atmosphere. The silicon oxycarbides evidence oxidative degradation that limits their lifetime as composite matrices. The present study characterizes bonding rearrangements in the oxycarbide network accompanying increases in pyrolysis temperature. It also addresses the changes in susceptibility to oxidation due to variations in the distribution of Si bonded species obtained under different processing conditions. The study is carried out using ^{29}Si nuclear magnetic resonance (NMR) spectroscopy and a design of experiments approach to model the oxidation behavior. The NMR results are compared with those obtained by thermogravimetric analysis (TGA). Samples pyrolyzed under inert conditions are compared to those pyrolyzed in reactive ammonia environments.

Keywords: silicon oxycarbide, Blackglas™, ceramic matrix composites, ^{29}Si NMR, oxidation

1. Introduction

Silicon oxycarbide glasses are characterized by Si, C, and O atoms bonded in an amorphous network. The network structure is dependent upon the thermal history of the material, and can undergo further redistribution with continued heating and higher temperature exposures.[1-7] Free carbon, presumed to inhibit the crystallization of silica and to be susceptible to diffusion and oxidation, may be present.[6,8] The properties of the glass, including its oxidation resistance, are expected to be controlled by the network structure and carbon content. Hence, understanding the development of this structure and its control are of importance in optimizing material behavior.

The system selected for study was Blackglas™ (Allied Signal, Inc.), chosen for its commercial availability and relatively low cost, and because of the growing interest in its use as a matrix precursor for ceramic matrix composites (CMCs). Long term use of Blackglas™ CMC components under cyclic oxidizing conditions requires an understanding of microstructural control, and ability to tailor the microstructure to optimize environmental durability.

Exposure of Blackglas™ CMCs at 600 °C in air typically is accompanied by loss of carbon from the matrix, and change in matrix color from black to white and translucent. To illustrate, an optical micrograph of a polished section of an aged Nextel 312 /BN/ Blackglas™ composite is shown in Figure 1. This micrograph reveals the depletion of carbon from the matrix as a change in color and reflectivity. The "whiter" island areas of

the matrix, as seen in an optical microscope, are higher in carbon than the darker gray matrix areas surrounding them, suggesting loss of carbon from the matrix through microcracks. Examination of matrix material alone is necessary to explain the observed composite oxidation.

The Blackglas™ polymer is produced by the catalyzed thermal polymerization of cyclosiloxanes and vinyl cyclosiloxanes through a hydrosilation reaction involving Si-H and vinyl groups, followed by pyrolysis in an inert environment.[9-11] Phenyl containing monomers, often used in producing "black glass" materials, and which contribute to free carbon in the oxycarbide glass, are absent in this material. The polymerization kinetics and pyrolysis reactions are discussed in detail by others.[12,13] [14] While this is not a "sol-gel" approach to forming oxycarbide glasses, and no solvent is used, the redistribution reactions observed in the oxycarbide network merit comparison with sol-gel derived materials.

In a prior study of Blackglas™,[7] samples that were pyrolyzed to 900°C for 15 minutes, exhibited poorer oxidation resistance than desired. It was proposed that this was due to incomplete pyrolysis, or to formation of Si moieties susceptible to continuing oxidation. Hence, the samples were further exposed to final temperatures of 1000 to 1400°C by reheating in argon, and characterized by ^{29}Si NMR. Additional samples pyrolyzed in flowing nitrogen to final temperatures of 800, 900 and 1000°C for 1 and 5 hours were examined using thermogravimetric analysis. It was shown from this study that pyrolysis at higher temperatures did change the relative distribution of Si species produced, and affected the susceptibility to oxidation.

The current study focuses on a more rigorous characterization of the pyrolyzed oxycarbide using ^{29}Si nuclear magnetic resonance (NMR) to delineate network structure. Changes in the structure due to oxidation also are followed by NMR in an effort to relate the oxidative stability to pyrolysis conditions. Inert (nitrogen) and reactive (ammonia) pyrolysis environments are examined. Statistical experimental design methods are used throughout this study to examine the relationship between pyrolysis conditions, silicon species formed and oxidation resistance.[15,16] Preliminary data have been presented at several technical conferences; this paper enables all of the data, plus additional results, to be analyzed together.

2. Experimental

2.1 ^{29}Si NMR

As pyrolyzed and oxidized samples were characterized by NMR using a Bruker AM-300 spectrometer controlled by a TECMAG data system running MACNMR 5.1 to 5.3 software. Solid samples were run with magic angle spinning at 5 kHz (MAS). Spectra were externally referenced to the ^{29}Si peak of the sodium salt of 3-trimethylsilylpropionic acid (0 ppm). Because of the long relaxation time of ^{29}Si and the need for near quantitative results, a short 2.5 ms pulse (~30° pulse angle) and 60 second delays were employed. To obtain good signal-to-noise ratios, 6000 scans were accumulated on each sample. Line fitting was conducted using simulation software available with MACNMR to determine percentage of each silicon species.

2.2 Preliminary assessment of line fitting

Before entering into a large study, it was necessary to assess whether ^{29}Si NMR could serve as a quantifiable means to follow the reactions occurring during pyrolysis. To this end, two samples were pyrolyzed at 1000°C for 1 hour. Peak areas (shown in Table 1,

runs 1 and 2) showed good agreement between spectra, with the peak areas for each Si species varying over only a 4 percent range. Therefore, it was determined that ^{29}Si NMR was a quantifiable tool to use for this study, and these first two runs were included in the final analysis of the data.

2.3 Phase 1: Experimental design for study of pyrolysis time and temperature

Previous studies served to identify two variables of probable importance to the formation of various Si tetrahedral species and their stability toward oxidation of the Blackglas™ material: pyrolysis time and temperature. In the current study, we wished to evaluate both the first and second order effects of both of these variables and the effect of oxidation time, as well as any synergistic/interactive effects among the variables. To accomplish this with a minimum number of experiments, we used a face-centered central composite experimental design. Three levels of time (1, 2.5 and 5 hours), three levels of temperature (900, 1000 and 1100°C), and three levels of oxidation time at 600°C (0, 250, and 500 hours) were investigated. The scope of the design can be described as a box with each of the three axes representing one of the three variables (as shown in Figure 2a). The experimental conditions run in this type of design include all eight corners of the box, the center of each of the six faces and the center of the box, for a total of 15 different experiments. This allows for statistical analysis of the responses (percentages of SiC_xO_{4-x} species present as determined by their relative peak areas in ^{29}Si NMR) in terms of pyrolysis time and temperature, and oxidation time, using a full quadratic model. This model can include all first and second order effects and all two-way interactions/synergistic effects for all three variables.

It is assumed in this type of design that experimental error is the same throughout the design space. Thus, three repeats of the conditions at the center of the box were run to quantify experimental reproducibility. From this, the significance of effects, as well as model adequacy and reliability, could be judged. A total of 18 experiments was carried out. In all experiments, samples were pyrolyzed in separate runs in a randomized run order to negate the effect of any systematic error. In the analysis of the data, these 18 runs (numbered 3-20 in Table 1) were used together with the 2 runs from the preliminary assessment of reproducibility to develop empirical models.

2.4 Phase 2: Pyrolysis atmosphere

A follow-up study was carried out to investigate the effects of pyrolysis atmosphere on the formation of various Si tetrahedral species and their stability toward oxidation. In this phase, three variables at two levels each, pyrolysis atmosphere (100 percent nitrogen or 100 percent ammonia), pyrolysis temperature (900 and 1000°C) and oxidation time (0 and 1000 hours) were investigated. Again, experimental design strategies were employed to greatly reduce the number of experiments. A fractional factorial design consisting of 4 distinct experiments each repeated twice was planned. The design can be described as a box with each of the three axes representing one of the three variables, as shown in Figure 2b. Half of the corners of the box are run. This is a frugal design meant to screen the relative importance of the main effects on the measured responses only.

2.5 Sample preparation

Samples of Blackglas™ 493A with 2 weight percent catalyst 493B added, cured at 55°C for 3 hours and post-cured at 150°C for 2 hours, were prepared by Allied Signal, Inc. In

the first phase of this study, 5-10g samples were pyrolyzed under flowing nitrogen (2L/min.) to final temperatures of 900, 1000 and 1100°C, and held at the highest temperature for 1, 3 or 5 hours. Pyrolysis yields ranged from 81.7 to 82.5 percent, with yield decreasing slightly with pyrolysis temperature. The small decrease in yield with increasing pyrolysis temperature is likely the result of hydrogen elimination; however, hydrogen content was not determined. Total carbon content in the as-pyrolyzed samples, as measured by elemental analysis, ranged from 25.29 to 27.56 weight percent.

The pyrolyzed material was ground to -200, +325 mesh to control surface area prior to oxidative exposure. The black powders were dried at 150°C overnight, then oxidized in flowing air at 600°C for periods of 0, 250 and 500 hours. The appearance of the powders pyrolyzed at 900°C changed dramatically following oxidation, becoming nearly white after 500 h. The 1000°C pyrolyzed samples were dark gray, while the 1100°C materials were still almost black after 500 h of oxidation. Weight changes after 500 hours of oxidation ranged from -1.42 % in the 900°C pyrolyzed material to +0.49 % in the 1100°C sample.

2.6 Thermogravimetic analysis

Thermogravimetric analyses (TGA) of the as-pyrolyzed materials were run to determine their susceptibility toward oxidation. A heating rate of 10°C/minute in flowing air at a flow rate of 60 cc/min was used in all of the runs.

3. Results

3.1 Study of redistribution reactions in inert atmosphere

A typical ^{29}Si NMR spectrum of Blackglas™ pyrolyzed in inert atmosphere is shown in Figure 3. The spectra consist of five peaks corresponding to silicon bonded to x carbon atoms and 4 - x oxygen atoms (where x = 0 to 4), according to assignments made by Babonneau et al.[4] and labeled in the figure. Typical ^{29}Si NMR spectra of Blackglas™ samples of 900 and 1100 °C pyrolyzed specimens are presented in Figure 4. The relative amounts of each of the silicon species appeared to change with changing pyrolysis and oxidation conditions. To quantify these changes, the relative peak areas were estimated by line fitting for all of the experimental runs. These peak areas for the SiC_4, SiC_2O_2, $SiCO_3$, and SiO_4 species are shown in Table 1. The SiC_3O peak was also used in the peak fitting, but varied randomly between 0 and 4 percent for all the runs, with no statistically significant relationship to any of the variables. Therefore, this peak is omitted from further discussion.

Figure 5 shows a graph of peak areas of the as-pyrolyzed materials as a function of pyrolysis temperature. From this graph, it is already evident that there is a large effect of pyrolysis temperature on the silicon redistribution reactions. The relative amounts of SiC_4 and SiO_4 moieties increased with increasing pyrolysis temperature, while the peak areas of other Si species diminished. The relative peak areas of samples pyrolyzed for 1 hour (closed symbols) appear nearly identical to those pyrolyzed for longer times (open symbols). This suggests that there is little or no effect of pyrolysis time on the relative peak areas.

The percent carbon in the silicon oxycarbide network can be estimated from the NMR peak areas. This assumes that (1) the total number of network carbons, C, can be accounted for by the equation: C = 3/4 (SiC_3O peak) + (SiC peak) + 1/2 (SiC_2O_2 peak) + 1/4 ($SiCO_3$ peak), and (2) total networked oxygens, O, can be accounted for by O = 1/2 (SiC_3O peak) + (SiC_2O_2 peak) + 3/2 ($SiCO_3$ peak) + 2(SiO4 peak), relative to networked silicon. The assumption is based on the valences of carbon, oxidation and silicon. In the as-pyrolyzed

samples, the networked carbon is estimated by NMR to account for between 17 and 21 percent of the silicon oxycarbide matrix. Total carbon content in the as-pyrolyzed samples, as measured by elemental analysis, ranged from 25.29 to 27.56 weight percent (Table 1). This difference between the percent carbon bound to silicon and the total carbon in the sample may be attributed to some combination of free carbon, carbon radicals, or carbon still bound to hydrogen.

3.2 Influence of network structure on oxidative stability

Comparison of as pyrolyzed samples with those following 500 h of oxidation time (Figure 6) shows the increase in SiO_4 groups with oxidative exposure, with some retention of oxycarbide species. The relative amounts of oxycarbide species maintained during oxidation was observed to increase with increasing pyrolysis temperature. To quantify the influence of pyrolysis time and temperature on oxycarbide structure, and furthermore, to examine the effect of this structure on the oxidative stability, the peak areas from all the experimental runs were analyzed by multiple linear regression. From this analysis, mathematical models could be derived for each Si species that describes the changes in peak area in terms of the statistically significant pyrolysis and oxidation conditions. It was determined in the analysis that log transformation of oxidation time before modeling resulted in the best fit to the experimental data for all peak areas. A 10-term full quadratic model of the form

$$response = A + B*PYTEMP + C*PYTIME + D*log(OXTIME) + E*PYTEMP^2 + F*PYTIME^2 + G*log(OXTIME)^2 + H*PYTEMP*PYTIME + I*PYTEMP*log(OXTIME) + J*PYTIME*log(OXTIME)$$

was entertained for each set of data. Terms not deemed statistically significant (<90 % confidence) were excluded from the model using the stepwise technique. Significant terms in the model and summary statistics are given in Table 3. These response surface models can be used to visualize the effects of the statistically significant variables on the response, as well as predict the conditions that produce the optimum properties. The predictive models found to best fit the data for all peak areas included terms for pyrolysis temperature, and log (oxidation time), but not pyrolysis time. In essence, pyrolysis time had no statistically significant effect on relative peak area.

The predictive model for percent SiC_4 peak contains first and second order terms for pyrolysis temperature and log oxidation time, as well as an interaction between the two variables. A 3-D graph of the predictive model plotted *versus* pyrolysis temperature and oxidation time is shown in Figure 6a. This graph clearly demonstrates that increasing pyrolysis temperature significantly increases the amount of SiC_4 moieties produced during pyrolysis. This increased silicon carbide production results in much improved oxidative stability, as evidenced by the greater retention of SiC_4 species after oxidation.

The predictive model for SiO_4 peak area also contains terms for pyrolysis temperature and log oxidation time, and an interaction between the two variables. Figure 6b shows a 3-D graph of the predictive model for percent SiO_4. Pyrolysis temperature had a dramatic effect on the amount of SiO_4 present both before and after oxidation. However, samples pyrolyzed at 1100 °C contained much less SiO_4 (~60%) than those pyrolyzed at 900 °C (100%), demonstrating the strong interaction between pyrolysis temperature and oxidation time.

Predictive models for the oxycarbide species $SiCO_3$ and SiC_2O_2, (Figures 6c and 6d, respectively) contain a smaller, though still statistically significant, relationship with pyrolysis time. Nevertheless, a strong interaction/synergistic effect between pyrolysis temperature and log oxidation time still is evident. The higher the pyrolysis temperature, the smaller the change in peak areas for $SiCO_3$ and SiC_2O_2 on oxidation.

Slices of the surfaces shown in Figure 6a and b are plotted in 7a and b, respectively, along with the actual experimental data points. These plots visually demonstrate that the models fit the data quite well, and further illustrate the strong synergistic effect of pyrolysis temperature on the oxidative stability.

Total carbon content, as determined by elemental analysis, decreases with oxidation; however, the extent of the decrease varies with pyrolysis temperature and log oxidation time, and is greatest for material pyrolyzed at 900°C, and least for the 1100°C material (Figure 8). Slices of the surface shown in Figure 8 are plotted along with the actual experimental data points in Figure 9. Consistent with models derived from the NMR data, these slices also show a strong synergistic effect of pyrolysis temperature on the oxidative stability.

Further confirmation of enhanced oxidative stability with increased pyrolysis temperature is obtained from TGA results (Figure 10). Samples were pyrolyzed to the final temperatures indicated in argon, then examined in flowing air in a TGA. After 900°C pyrolysis, the samples first lose weight in air, then gain weight in the region between 400 and 800°C, then again lose weight. The extent of the weight change diminishes with pyrolysis time. For the sample pyrolyzed at 1100°C, weight is relatively constant throughout the run, indicative of enhanced oxidative stability, and in agreement with the NMR result.

3.3 Follow up study: Effect of ammonia atmosphere on redistribution reactions

The objective of this follow up study was to determine whether there is a difference in oxidative stability of silicon oxynitride as compared with silicon oxycarbide. The oxynitride species are expected to be produced by pyrolysis of the Blackglas™ in an ammonia atmosphere.[16-21] Under these conditions, a mixture of oxynitride species appears to be obtained as evidenced by ^{29}Si NMR.[21] There is no SiC_4 peak present in these mixtures. The $SiN_xO_{(4-x)}$ peaks that are present cannot be resolved from certain of the oxycarbide peaks ($SiCO_3$ and SiC_2O_2) observed in Blackglas™ pyrolyzed in nitrogen.

Typical ^{29}Si NMR results from this screening study are shown in Figure 11. In agreement with van Weeren et al.,[21] a mixture of oxynitride species is produced in ammonia atmosphere. Only SiO_4 could reliably be resolved from the other peaks in the ammonia pyrolyzed samples. The percent SiO_4 peak areas for each of the experimental design conditions are shown in Table 2. Initially, eight runs were planned. Unfortunately, in the 500 hour oxidized samples, stagnant air instead of flowing air was employed, and there was very little change in the ^{29}Si NMR for any of the oxidized samples. Subsequently, two of the 500 hour oxidized runs were repeated in flowing air (runs 9 and 10 in Table 2). A graph of this data is shown in Figure 12.

Mathematical models were derived for this data by multiple linear regression (omitting the stagnant air oxidation runs). Because a scant screening design was employed in the study, only the main effects of pyrolysis atmosphere (expressed as 0 to 100% ammonia concentration), pyrolysis temperature and oxidation time could be entertained in the model. Of these, only oxidation time and ammonia concentration were found to be statistically significant (see Table 3). Pyrolysis temperature was not found to have a statistically significant effect on SiO_4 peak area. However, this should be interpreted with some caution due to the limited number of samples in this screening study. Pyrolysis temperature may well have an effect in a more complete study.

The ammonia appears to react to diminish the formation of SiO_4 species during pyrolysis, as compared with the nitrogen pyrolyzed material (Figure 12). However, although less SiO_4 is produced initially, the rate of SiO_4 formation on oxidation appears to be the same as

that of the Blackglas™ pyrolyzed under inert conditions. Hence, for long term applications, there is no direct benefit from ammonia treatment. Since oxidation is considerably more rapid when reactants are removed by flowing air than in the stagnant air oxidation environment, actual lifetimes will depend on application.

4. Discussion

Pyrolyzed Blackglas™ samples exhibit all possible tetrahedral species of silicon bonded to carbon and oxygen. However, the relative distribution of these species is dependent most strongly on pyrolysis temperature, and less on pyrolysis time. The oxycarbide structure is metastable, and undergoes rearrangement to the more thermodynamically stable SiC_4 and SiO_4 groups, as is observed in sol-gel derived oxycarbide glasses. The data obtained here indicate that the higher the initial pyrolysis temperature, the greater the relative concentrations of SiC_4, and the more oxidatively stable the material. Higher pyrolysis temperatures also produce lesser relative concentrations of SiC_2O_2 and $SiCO_3$. Although the SiC_4 species is susceptible to oxidation, it is oxidized more slowly than SiC_2O_2 or $SiCO_3$ groups, as would be expected based on steric hindrance. The finding of improved oxidation resistance with higher pyrolysis temperature is consistent with that observed for polymers of methyltrimethoxysilane produced by sol-gel synthesis.[22] The present studies were conducted on powders to maintain a consistent surface to volume ratio. In composites, however, diffusion, matrix microcracking, and matrix densification with increasing temperature also must be considered. For composites reinforced with Nextel 312 fiber, composite processing temperatures are limited to nominally 1000°C so as to avert fiber degradation. Therefore, although the 1100°C pyrolysis temperature is the optimum one in terms of matrix properties, it cannot be applied to this composite system.

5. Conclusions

Pyrolysis temperature and atmosphere determine the silica species present in the oxycarbide network. The network structure influences the oxidative stability. Pyrolysis at 1100°C, the highest temperature studied here, produces the most oxidatively stable ceramic material. For samples with large surface-to-volume ratios, there is no benefit in pyrolyzing for more than one hour. Shorter pyrolysis cycles can greatly reduce production costs of the ceramic part, but the influence of time would need to be re-evaluated in fabrication of thick parts. Pyrolysis in ammonia results in less silica formation in the as-pyrolyzed material than occurs in an argon environment, based on preliminary screening results. However, oxidative exposure results in an increase in SiO_4 at the same rate regardless of pyrolysis atmosphere. Hence, ammonia pyrolysis does not appear to offer a solution for parts where an extended performance life under oxidizing conditions is required. It should be noted that the above conclusions are based on optimization of matrix properties alone. For a Blackglas™ composite, establishing pyrolysis conditions for maximizing oxidative stability must also take into account the particular fiber and interphase used, as these can limit processing temperatures.

Acknowledgment

The authors wish to thank Drs. Stephen T. Gonczy, Roger Leung (Allied Signal, Inc.), Dr. Philip Adler (Northrop Grumman Corp.) for supplying samples, and Terrance Kacik (Cleveland State University) for carrying out thermal analysis.

References

1. V. Belot, R. J. P. Corriu, D. Leclercq, P. H. Mutin, A. Vioux, "Thermal reactions occurring during pyrolysis of crosslinked polysiloxane gels, precursors to silicon oxycarbide glasses," *Journal of Non-Crystalline Solids* **147-148**, 52-55 (1992).

2. V. Belot, R. J. P. Corriu, D. Leclercq, P. H. Mutin, A. Vioux, "Silicon oxycarbide glasses with low O/Si ratio from organosilicon precursors," *Journal of Non-Crystalline Solids* **176**, 33-44 (1994).

3. V. Belot, R. J. P. Corriu, D. Leclercq, P. H. Mutin, A. Vioux, "Redistribution reactions in silsesquioxane gels," *Journal of Materials Science Letters* **9**, 1052-1054 (1990).

4. F. Babonneau, L. Bois, C.-Y. Yang, L. V. Interrante, "Sol-gel synthesis of a siloxypolycarbosilane gel and its pyrolytic conversion to silicon oxycarbide," *Chemistry of Materials* **6**, 51-57 (1994).

5. L. Bois, J. Maquet, F. Babonneau, H. Mutin, D. Bahloul, "Structural characterization of sol-gel derived oxycarbide glasses. 1. Study of the pyrolysis process.," *Chemistry of Materials* **6**, 796-802 (1994).

6. F. I. Hurwitz, P. Heimann, S. C. Farmer, J. D. M. Hembree, "Characterization of the pyrolytic conversion of polysilsesquioxanes to silicon oxycarbides.," *Journal of Materials Science* **28**, 6622-6630 (1993).

7. F. I. Hurwitz, P. Heimann, T. A. Kacik, "Redistribution reactions in Blackglas™ during pyrolysis and their effect on oxidative stability.," *Ceramic Engineering and Science Proceedings* **16**, 217-224 (1995).

8. H. Zhang, C. G. Pantano, "Synthesis and characterization of silicon oxycarbide glasses," *Journal of the American Ceramics Society* **73**, 958-963 (1990).

9. R. Y. Leung, S. T. Gonczy, M. S. Shum, "Carbon-containing black glass monoltihs", Patent US 5,242,866, Sep. 7, 1993.

10. R. Y. Leung, S. T. Gonczy, "Process for preparing black glass using cyclosiloxane precursors", Patent US 5,231,059, Jul. 27, 1993.

11. R. Y. Leung, W. D. Porter, "Curing and pyrolysis of Blackglas™ resins and composites," *Ceram. Eng. Sci. Proc.* **17**, 386-393 (1996).

12. J. P. Dunkers, R. S. Parnas, "An infrared attenuated total refelction cure monitor for control of the liquid composited molding process," *Ceram. Eng. Sci. Proc.* **16**, 201-208 (1995).

13. J. Annamalai, W. N. Gill, A. Tobin, "Modeling, analysis and kinetics of transformation in Blackglas™ preceramic polymer pyrolysis," *Ceram. Eng. Sci. Proc.* **16**, 225-232 (1995).

14. W. N. Gill, et al., "Development of a mechanistic model for Blackglas™ pyrolysis: comparison of theory and experiment," *Ceram. Sci. Eng. Proc.* **18** (1997).

15. M. A. B. Meador, F. I. Hurwitz, G. S. T, "NMR study of redistribution reactions in Blackglas™ and their influence on oxidative stability.," *Ceram. Eng. Sci. Proc.* **17**, 394-400 (1996).

16. R. Y. Leung, M. Glazier, M. A. B. Meador, "Synthesis and thermal stability of nitrogen-containing Blackglas™ ceramic," *Ceram. Eng. Sci. Proc.* **18** (1997).

17. R. M. Laine, Y. D. Blum, R. D. Hamlin, A. Chow, "Organometallic polymers as precursors to ceramic materials: Silicon nitride and silicon oxynitride," in *Ultrastructure Processing of Advanced Ceramics* D. D. Mackenzie, D. R. Ulrich, Eds. (J. Wiley and Sons, New York, 1988) pp. 761-769.

18. Y. D. Blum, "Hydridosiloxane precursors for ceramic manufacture", Patent US Patent 5,128,494, July 7, 1992.

19. M. Sekine, S. Katayama, M. Mitomo, "Preparation of silicon oxynitride glass fibers by ammonolysis of silica gels," *J. Non-Cryst. Solids* **134**, 199-207 (1991).

20. R. K. Brow, C. G. Pantano, "Thermochemical nitridation of microporous silica films in ammonia," *J. Am. Ceram. Soc.* **70**, 9-14 (1987).

21. R. van Weeren, E. A. Leone, S. Curran, L. C. Klein, S. C. Danforth, "Synthesis and characterization of amorphous Si_2N_2O," *J. Am. Ceram. Soc.* **77**, 2699-702 (1994).

22. H. Zhang, C. G. Pantano, High temperature stability of oxycarbide glasses, M. J. Hampden-Smith, W. G. Klemperer, C. J. Brinker, Eds., Better Ceramics Through Chemistry V, San Francisco, CA (Materials Research Society, 1992).

List of figures

Table 1. Experimental conditions and NMR peak areas for pyrolysis study

Run Order	*Pyrolysis temp., °C*	*Pyrolysis time, hours*	*Oxidation time, hours*	*Percent SiC_4*	*Percent SiC_2O_2*	*Percent $SiCO_3$*	*Percent SiO_4*	*Percent Carbon**
1	1000	1	0	27.48	26.22	25.21	20.12	
2	1000	1	0	29.71	24.83	24.80	17.33	
3	900	1	0	22.89	31.71	27.56	14.80	26.72
4	1100	1	0	37.97	16.27	21.15	23.43	26.8
5	1000	3	250	12.08	12.95	8.31	65.97	
6	900	5	0	26.31	31.07	26.51	14.45	27.46
7	1000	3	250	15.15	10.27	10.98	58.96	15.11
8	1100	5	0	35.31	16.91	19.73	25.34	26.56
9	1000	3	0	28.95	24.58	24.56	18.62	25.29
10	1100	1	500	16.04	10.61	8.98	62.83	12.2
11	900	5	500	0.26	0.86	0.18	98.96	2.8
12	1100	5	500	19.79	10.47	10.86	57.00	15.5
13	900	3	250	4.16	0.01	0.89	94.95	3.73
14	1100	3	250	23.20	10.56	12.33	49.83	18.56
15	1000	3	250	11.07	11.32	7.94	68.53	
16	1000	1	250	9.77	9.29	9.27	68.75	11.74
17	1000	5	250	13.11	13.46	9.95	60.19	14.51
18	1000	3	500	6.91	9.18	6.05	76.38	6.83
19	900	1	500	0.00	0.01	0.01	100.00	0.64
20	1000	3	250	12.67	8.78	7.74	68.67	13.43

*determined by elemental analysis

Table 2. Experimental conditions and NMR peak areas for follow-up screening study.

Run Order	Pyrolysis atm, percent NH_3	Pyrolysis temp, °C	Oxidation time, hours	Oxidation atm	Percent SiO_4
1	0	900	500	stagnant air	29.8
2	100	1100	500	stagnant air	9.83
3	100	900	0		11.98
4	100	1100	500	stagnant air	10.11
5	0	900	500	stagnant air	23.8
6	0	1100	0		22.2
7	0	1100	0		24.33
8	100	900	0		6.95
9	100	1100	500	flowing air	30.86
10	0	900	500	flowing air	45.3

Table 3. Summary statistics for predictive models.

Experimental Design	*Response*	*Model Terms (% Significance)*	*Residual df*	*Standard error of estimate*	R^2
Phase 1	SiC_4	TEMP (99.99) $TEMP^2$ (94.94) log(OXTIME) (99.99) $log(OXTIME)^2$ (98.18) TEMP x log(OXTIME) (98.76)	14	1.63	0.98
	$SiCO_3$	TEMP (99.52) $TEMP^2$ (99.66) log(OXTIME) (99.99) TEMP x log(OXTIME) (99.99)	15	1.05	0.99
	SiC_2O_2	$TEMP^2$ (99.92) log(OXTIME) (99.99) TEMP x log(OXTIME) (99.99)	16	1.81	0.97
	SiO_4	TEMP (99.99) $TEMP^2$ (98.69) log(OXTIME) (99.99) TEMP x log(OXTIME) (99.99)	15	3.94	0.98
Phase 2	SiO_4	% AMMONIA (99.54) OXTIME (99.85)	3	2.24	0.98

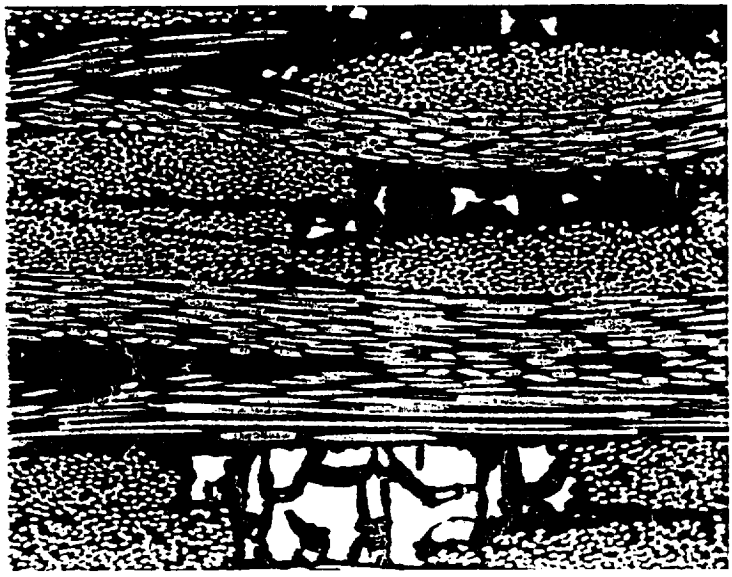
100 µm

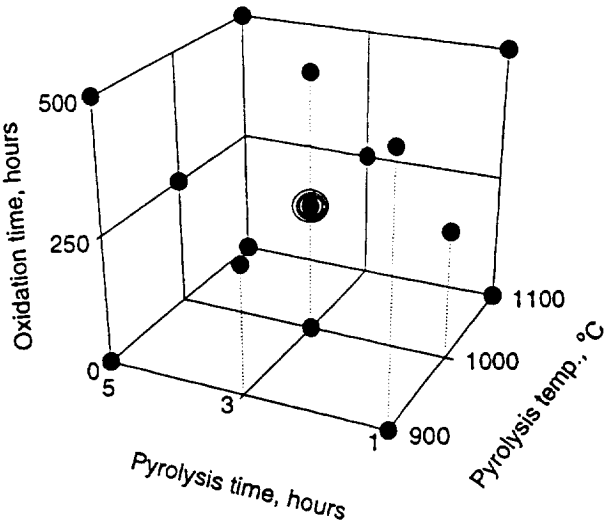
Oxidation time, hours
500
250
0
5
3
1
Pyrolysis time, hours
900
1000
1100
Pyrolysis temp., °C

a.

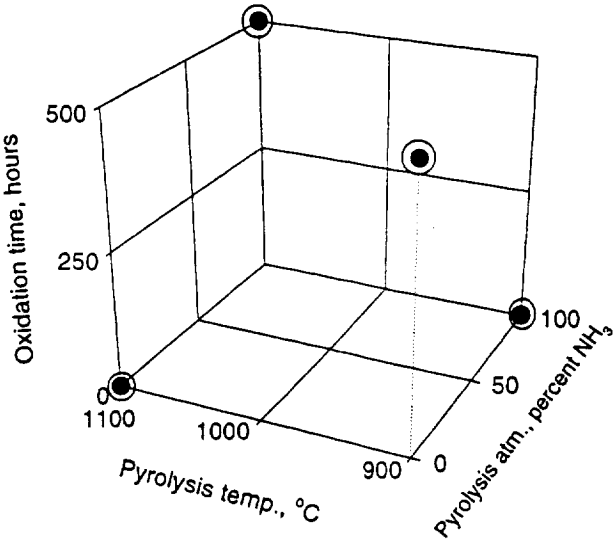
Oxidation time, hours
500
250
0
1100
1000
900
Pyrolysis temp., °C
0
50
100
Pyrolysis atm., percent NH_3

b.

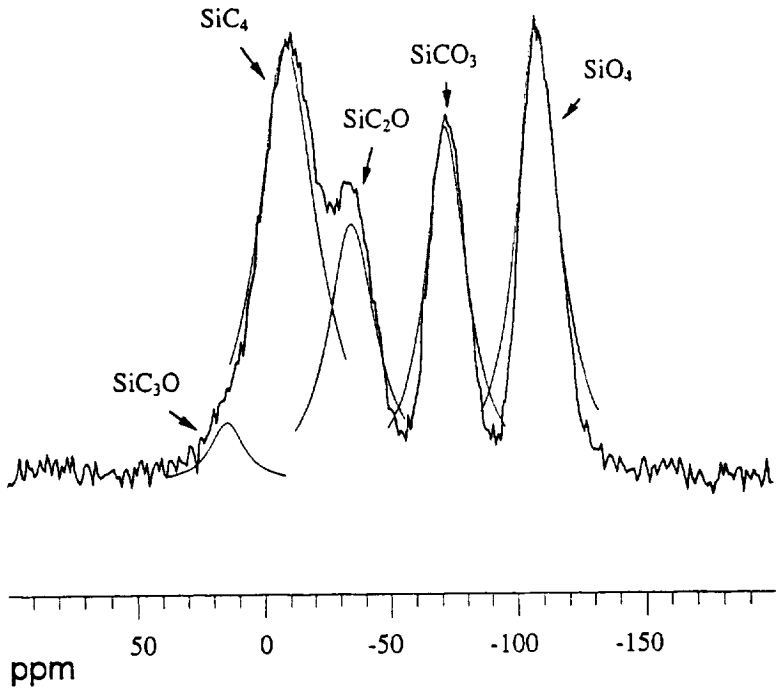
SiC4
SiCO3
SiO4
SiC2O
SiC3O
50
0
-50
-100
-150
ppm

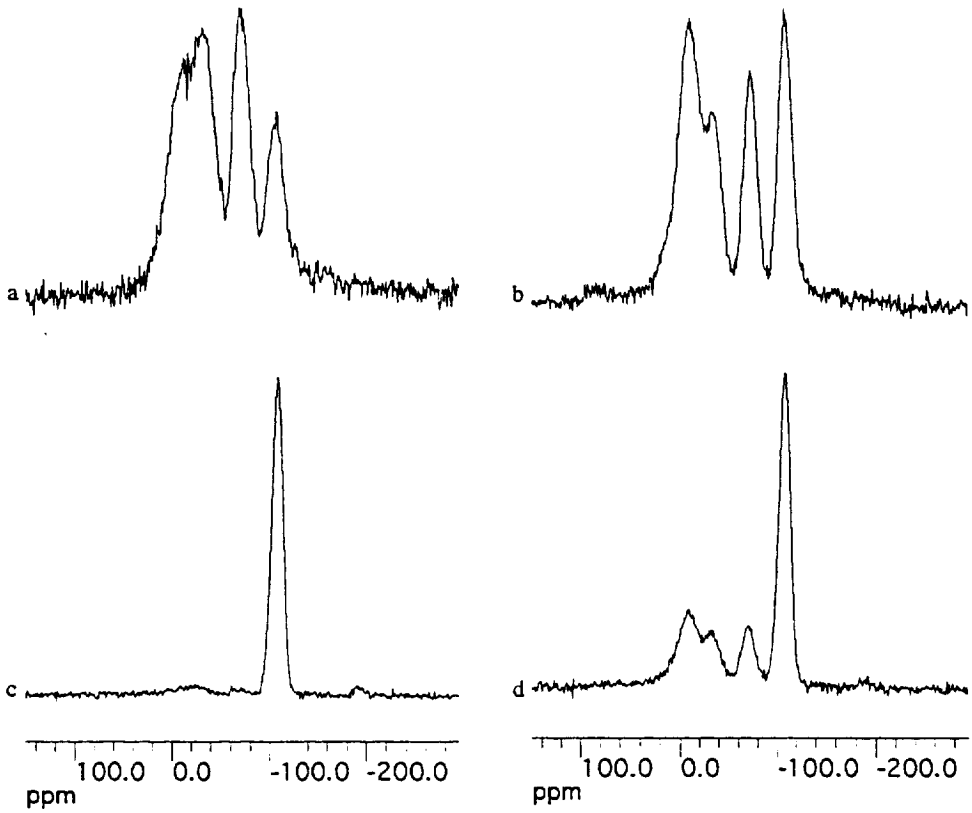
a
b
c
d
100.0
0.0
-100.0
-200.0
ppm
100.0
0.0
-100.0
-200.0
ppm

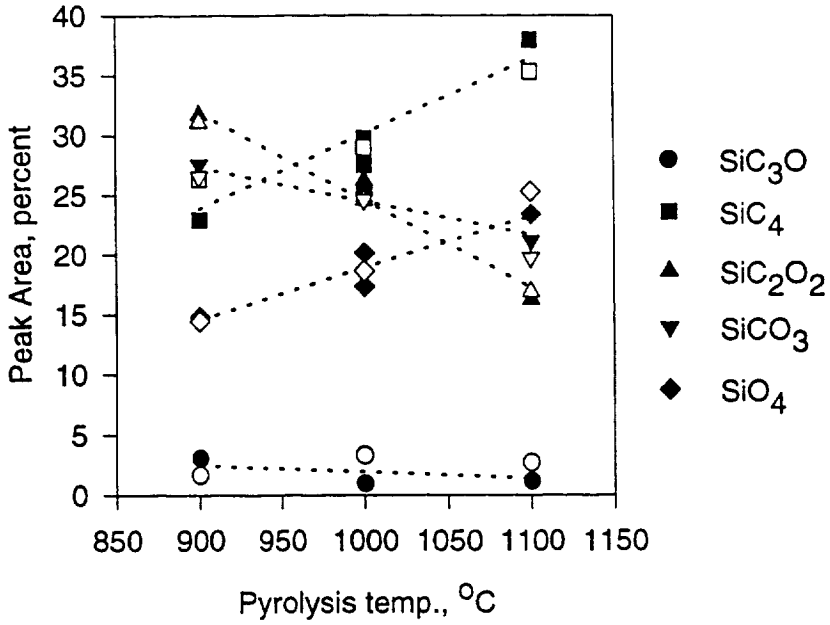
40
35
30
25
20
15
10
5
0
Peak Area, percent
850
900
950
1000
1050
1100
1150
Pyrolysis temp., °C
SiC3O
SiC4
SiC2O2
SiCO3
SiO4

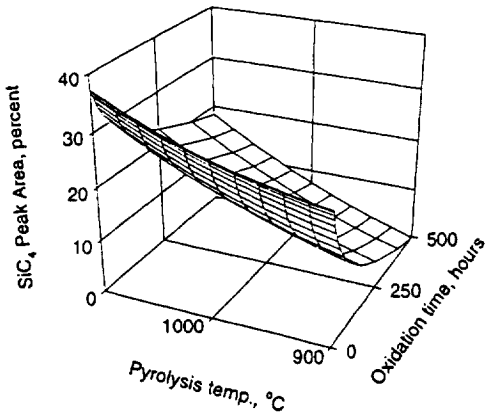
SiC_4 Peak Area, percent
40
30
20
10
0
1000
900
Pyrolysis temp., °C
0
250
500
Oxidation time, hours

a.

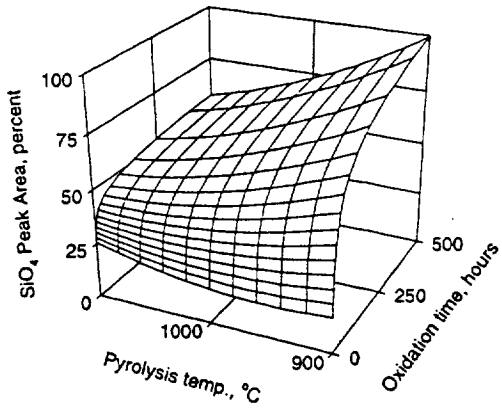
SiO_4 Peak Area, percent
100
75
50
25
0
1000
900
Pyrolysis temp., °C
0
250
500
Oxidation time, hours

b.

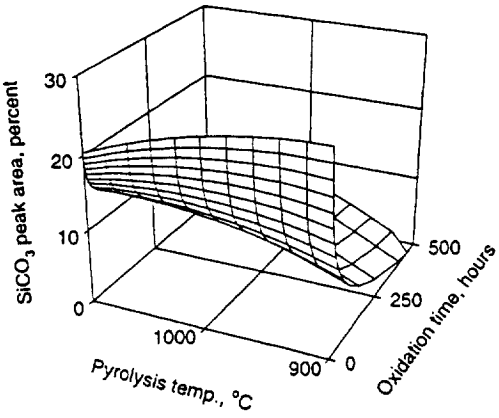
$SiCO_3$ peak area, percent
30
20
10
0
1000
900
Pyrolysis temp., °C
0
250
500
Oxidation time, hours

c.

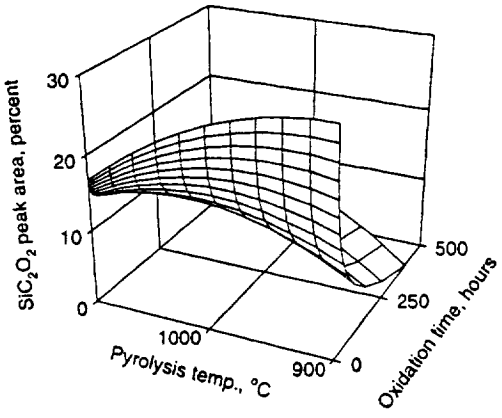
SiC_2O_2 peak area, percent
30
20
10
0
1000
900
Pyrolysis temp., °C
0
250
500
Oxidation time, hours

d.

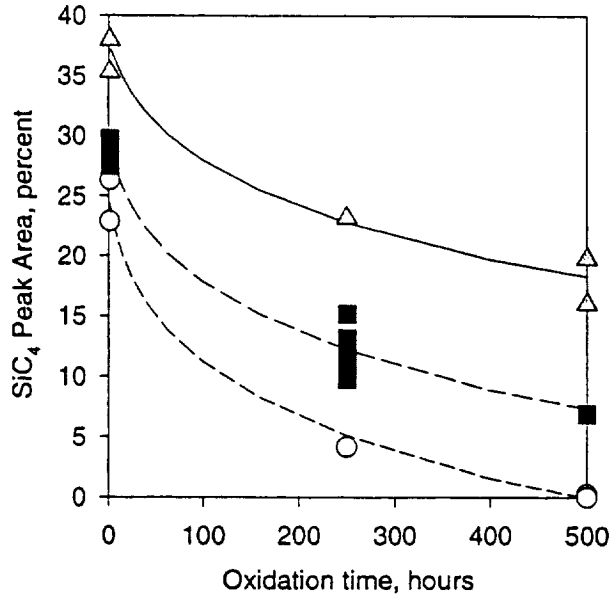
40
35
30
25
20
15
10
5
0
SiC_4 Peak Area, percent
0
100
200
300
400
500
Oxidation time, hours

a.

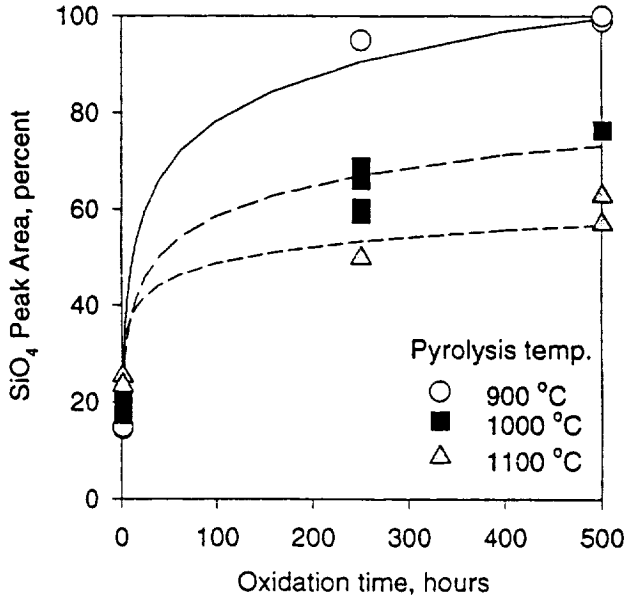
100
80
60
40
20
0
SiO_4 Peak Area, percent
Pyrolysis temp.
900 °C
1000 °C
1100 °C
0
100
200
300
400
500
Oxidation time, hours

b.

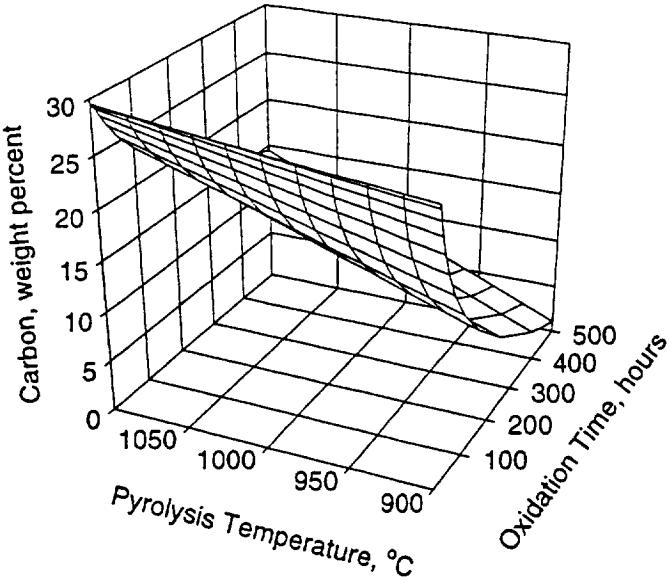
Carbon, weight percent
30
25
20
15
10
5
0
1050
1000
950
900
Pyrolysis Temperature, °C
500
400
300
200
100
Oxidation Time, hours

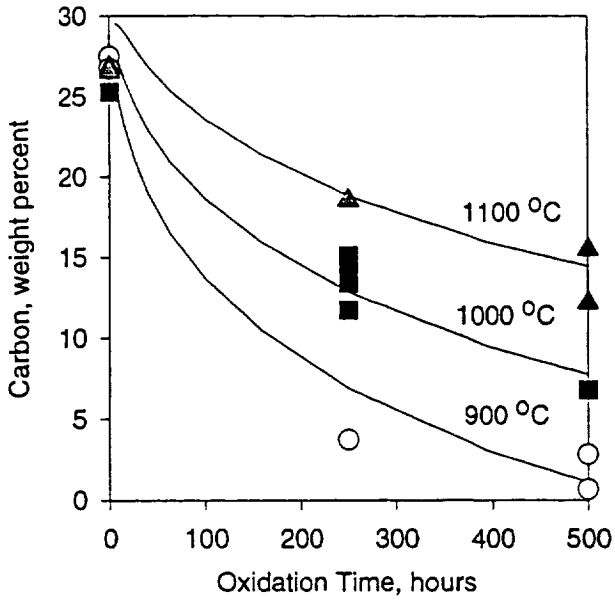
30
25
20
15
10
5
0
Carbon, weight percent
1100 °C
1000 °C
900 °C
0
100
200
300
400
500
Oxidation Time, hours

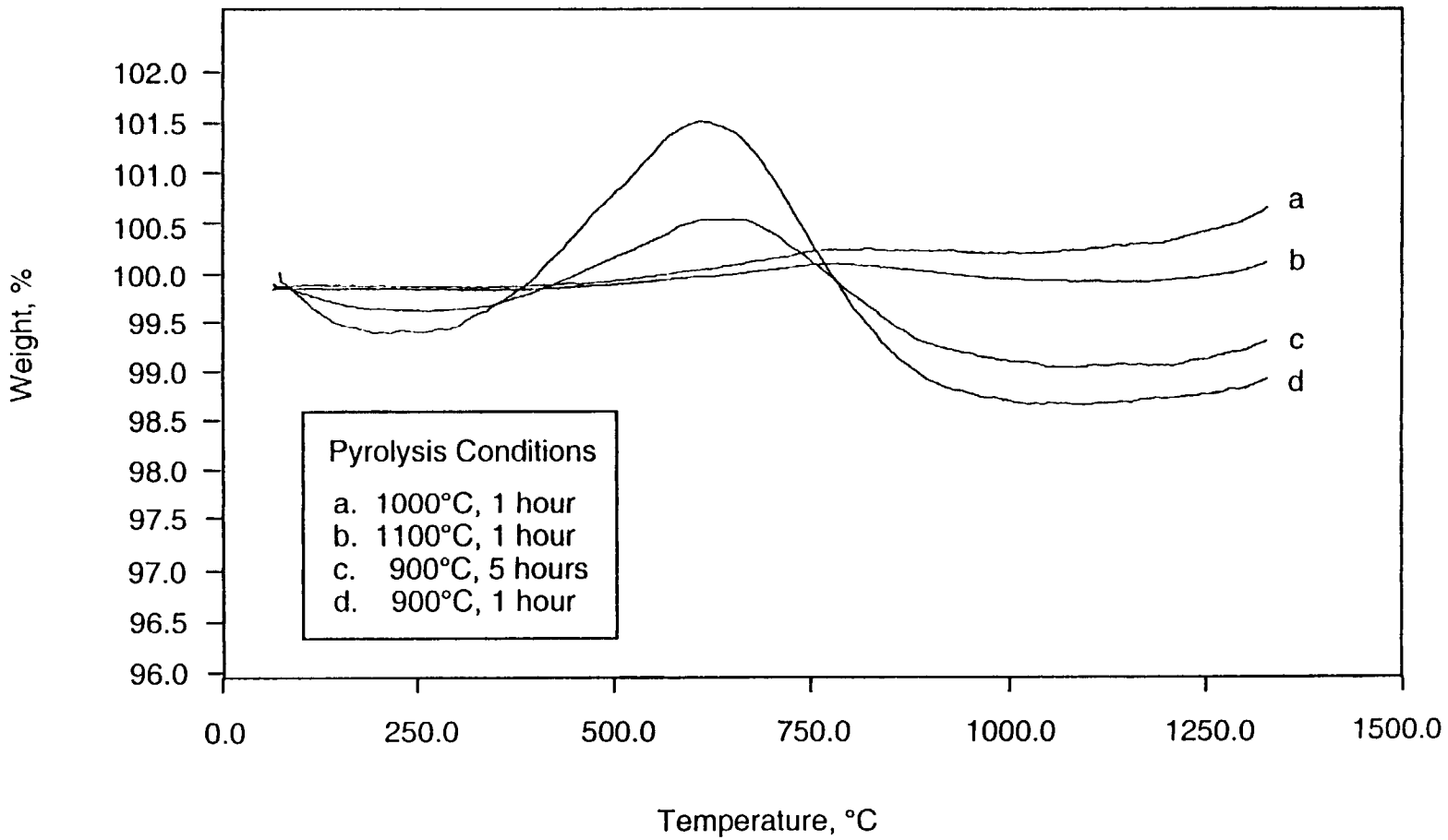
Weight, %
102.0
101.5
101.0
100.5
100.0
99.5
99.0
98.5
98.0
97.5
97.0
96.5
96.0
0.0
250.0
500.0
750.0
1000.0
1250.0
1500.0
Temperature, °C
a
b
c
d
Pyrolysis Conditions
a. 1000°C, 1 hour
b. 1100°C, 1 hour
c. 900°C, 5 hours
d. 900°C, 1 hour

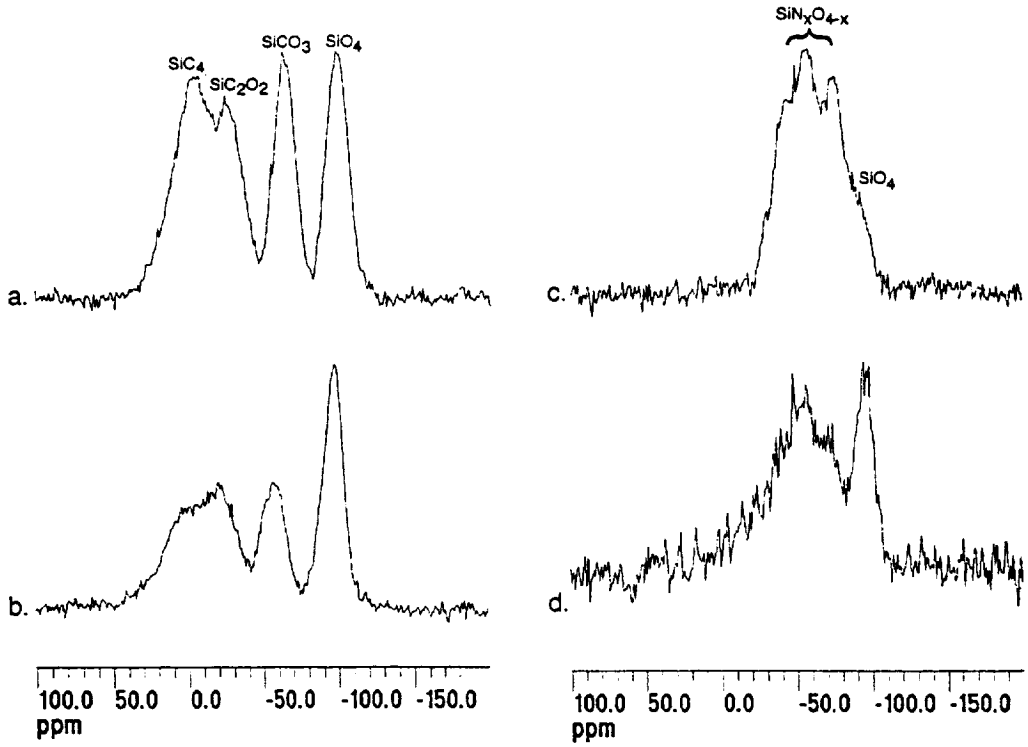
a.
b.
c.
d.
SiC_4
SiC_2O_2
$SiCO_3$
SiO_4
SiN_xO_{4-x}
SiO_4
100.0 50.0 0.0 -50.0 -100.0 -150.0
ppm
100.0 50.0 0.0 -50.0 -100.0 -150.0
ppm

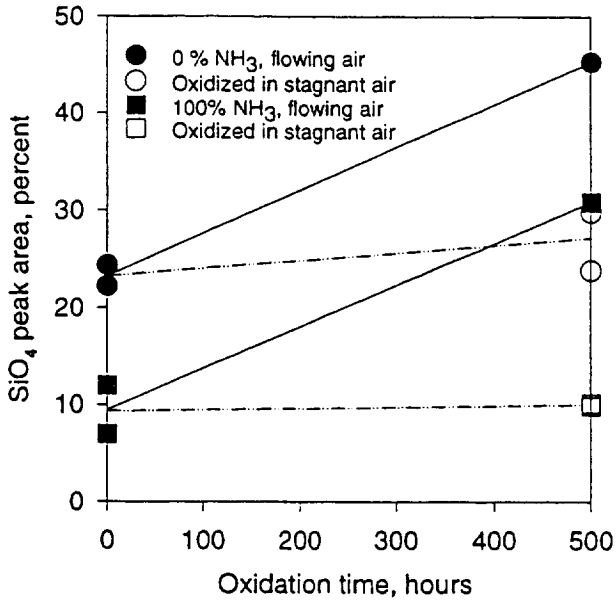
50
40
30
20
10
0
0
100
200
300
400
500
SiO_4 peak area, percent
Oxidation time, hours
0 % NH_3, flowing air
Oxidized in stagnant air
100% NH_3, flowing air
Oxidized in stagnant air